“Determination of the N protein of Nipah virus and its ligands as a potential new Anti-Nipah viral drug”

Submitted to

Department of Pharmacy

Faculty of Allied Health Sciences

Daffodil international university

Submitted by

Student Id: 183-29-141

Batch 20th DSC

Department of Pharmacy

Daffodil International University

Submission Date: 24 November 2022

Approval

This project paper, entitled **"Determination of the N protein of Nipah virus and its ligands as a potential new Anti-Nipah viral drug"** submitted to the Department of Pharmacy, Faculty of Allied Health Sciences, Daffodil International University, has been recognized as acceptable for the partial fulfillment of the requirements for the degree of Bachelor of Pharmacy (B. Pharm.) and approved as to its style and contents.

BOARD OF EXAMINES

……

Dr. Muniruddin Ahamed

Professor and Head **Chairman**

Department of pharmacy

Faculty of Allied Health Sciences

Daffodil International University

…….. **Internal Examiner**

…….. **Internal Examiner**

…….. **External Examiner**

Certificate

This is to certify that the results of the investigation that are embodied in this project are original and have not been submitted before in substance for any degree of this University. The entire present work submitted as a project work for the partial fulfillment of the degree of Bachelor of pharmacy, is based on the result of author's (Id: 183-29-141) own investigation.

SUPERVISED BY

Mr. Galib Muhammad Abrar Ishtiaque

Lecturer

Department of Pharmacy

Faculty of Allied Health Sciences

Daffodil International University

Declaration

I, Sabbir Ahmed, Id: 183-29-141, Department of Pharmacy, Daffodil International University, under the supervision of Mr. Galib Muhammad Abrar Ishtiaque, Lecturer, Department of Pharmacy, Faculty of Allied Health Sciences, hereby affirm that the work presented herein, entitled "Determination of the N protein of Nipah virus and its ligands as a potential new Anti-Nipah viral drug" represents my independent and thoughtful efforts toward completion of the requirements for the Bachelor of Pharmacy degree (B. Pharm.). I hereby claim that the content and ideas included in this work are mine. Also, I swear that I haven't turned in this project, or any portion of it, anywhere else to get my bachelor's or any other degree.

Md Sabbir Ahmed

Id: 183-29-141

Department of Pharmacy

Faculty of Allied Health Sciences

Daffodil International University

Dedication

Thank you to my family and teachers for always loving and supporting me through this process.

Acknowledgement

The first thing I want to do is offer thanks to Allah, the Almighty, for blessing me with the chance to study this topic and the skills to accomplish my project. I owe a lot of thanks to Mr. Galib Muhammad Abrar Ishtiaque, Lecturer, in the Department of Pharmacy. He was my project supervisor and gave me a lot of helpful advice and supervision throughout the course.

Thank you for the chance to collaborate on this project, Professor Dr. Muniruddin Ahamed, Head of the Department of Pharmacy at Daffodil International University. I'd also like to thank the other faculty and staff at DIU's Pharmacy Department for being helpful and let the instructors there know how much I appreciate them.

As a concluding point, I'd like to thank my father, mother, and other relatives for their helpful cooperation and support during this undertaking.

Md Sabbir Ahmed

Author

Abstract

The purpose of this research was to produce potential inhibitors of Nipah virus by first determining the full-length 3D structure of the N-protein of the virus. Methods for Molecular Modelling using the Nipah virus sequence from UniProt KB was used since its entire structure is not yet available in the Protein Data Bank (PDB). Templates with high levels of sequence similarity and coverage were found with the use of BLAST. The whole sequence of the Nipah virus N- protein was entered into the i-TASSER system, and after ab-initio modeling was used to combine loops with functional domains, five models were projected. These models were validated with the help of Ramachandran's evaluation. Using UCSF-Chimera, we severed the connections between the loops and the functional domains of the i-TASSER model. The in-house designed tool was used to assemble these loops and pieces. After the Swiss PDB viewer had minimized the binding energies, the CASTp server figured out where the ligands would go. Once binding pockets were identified, the e-LEA3D server assisted with the development of ligand molecule designs. With the goal of creating medications that effectively suppress the spread of Nipah virus in the future, the pharmacokinetic features of each of these ligands were analyzed in further depth on the Mobyle@RPBS online site.

Table of Content

List of Table

List of Figure

Chapter 1

INTRODUCTION

1. Introduction

1.1 General information Nipah Virus

Nipah virus (NiV) is a nonsegmented, single-stranded, negative-sense RNA virus that belongs to the family Paramyxoviridae and genus Henipavirus. NiV is a zoonotic virus (transmitted from animals to humans) and may also be spread directly between people or through tainted food. NiV was discovered in 1999 during a disease outbreak in pigs and humans in Malaysia and Singapore. This outbreak caused approximately 300 human cases and over 100 deaths [1]. Even though there haven't been any more cases in Malaysia since then, Bangladesh and India have occasionally experienced outbreaks. Since 2001, the Nipah virus has infected hundreds of people, with a 75% average mortality rate [2]. One of the deadliest viruses known to infect people is a zoonotic biosafety level 4 (BSL4) agent that, depending on the geographic regions of outbreaks, causes case fatality of between 40% and 100% in both humans and animals [3].

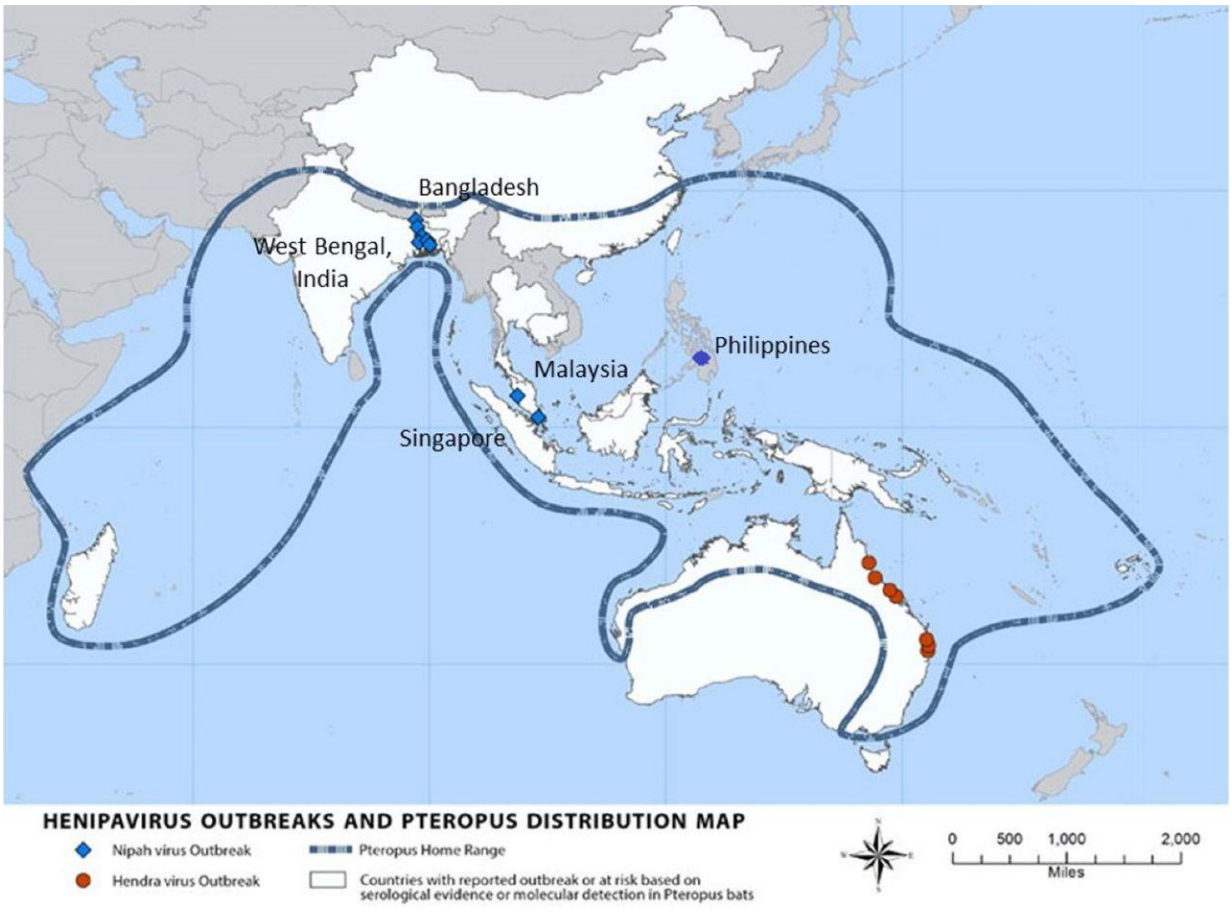

Figure 1.1.1: Henipavirus Outbreaks and Pteropus Distribution Map.

Research undertaken in Bangladesh from 2001 to 2021, there were a total of 322 cases, 229 fatalities, and a motality rate of 70% [4]. The worldwide prevalence of Nipah virus has been reported in about seven hundred cases and with a mortality rate of about 61.28% [5].

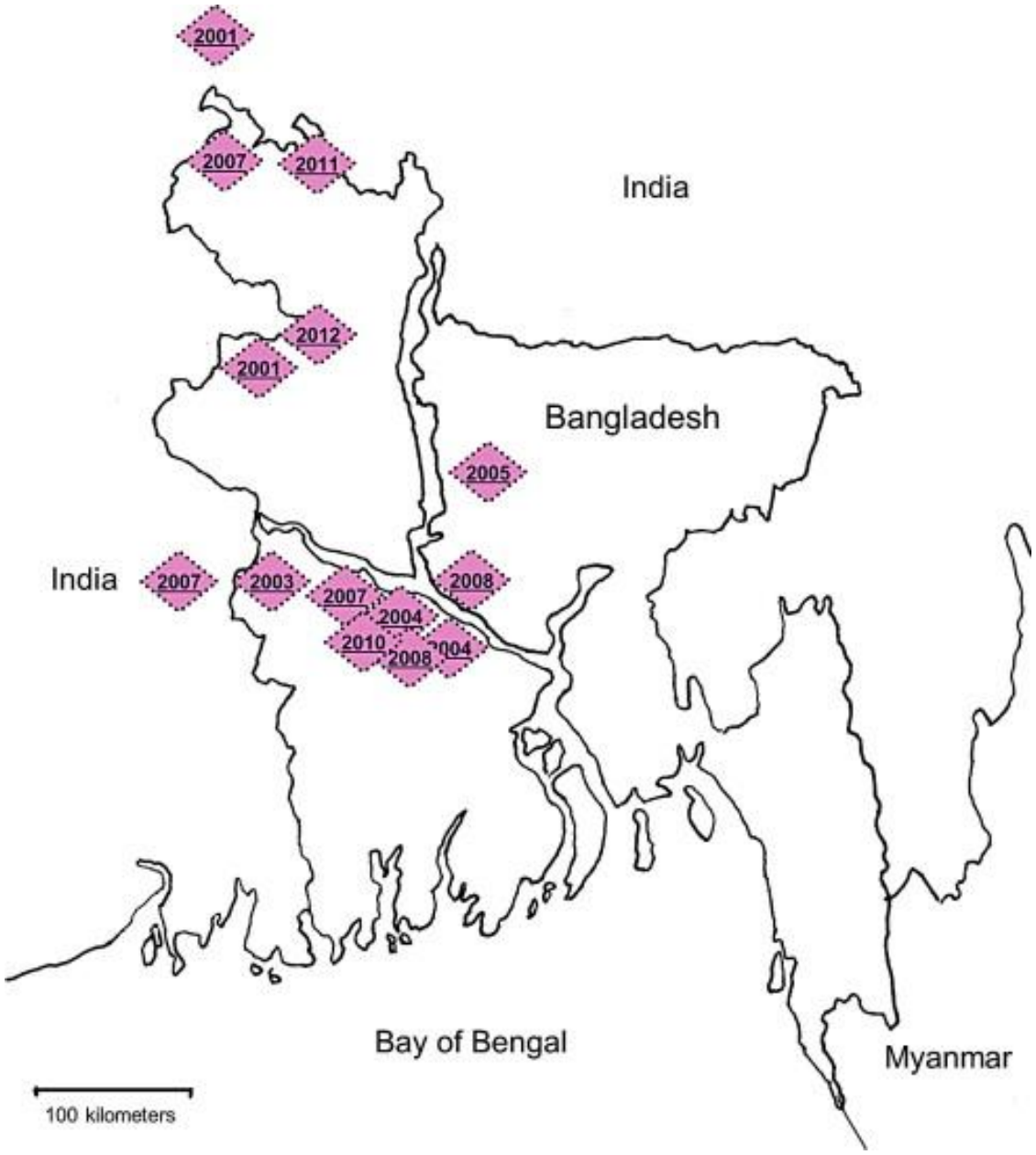

Figure 1.1.2: Date and location of Nipah outbreaks in Bangladesh

In the World Health Organization's (WHO) surveillance and outbreak alert report, it was evidently noted that better nursing and treatment facilities, along with public awareness campaigns, had not been able to lower the morbidity and mortality rates of Nipah virus infection, particularly during the winter and spring, which is thought to be the bats' breeding season and when they are most likely to spread the virus [6].

Table 1.1: Nipah virus outbreaks in Bangladesh

Yearly distribution of Nipah cases in Bangladesh 2001-2022				
Timeline	Case	Outlive	Death	Death rate in %
2001	13	4	9	69
2002	0	0	0	0
2003	12	4	8	67
2004	67	17	50	75
2005	12	1	11	92
2006	0	0	0	0
2007	18	9	9	50
2008	11	4	7	64
2009	4	3	1	25
2010	18	2	16	89
2011	43	6	37	86
2012	17	5	12	71
2013	31	6	25	81
2014	37	21	16	43
2015	15	4	11	73
2016	0	0	0	0
2017	3	1	2	67
2018	4	1	3	75
2019	8	1	7	88
2020	7	2	5	71
2021	2	2	0	0
2022	Not published	---------	----------	----------
Add up to	322	93	229	71%

1.2 Mode of Transmission

In contrast to Malaysia, where the outbreak spread from the natural host to an amplification host before contacting people, Bangladesh did not require an amplification host. Fruit bats were perhaps directly contaminating humans. Consumption of fruits or fruit products (such raw date palm sap) contaminated with the urine or saliva of infected fruit bats was the most likely cause of infection in the outbreaks in Bangladesh and India. Others who were engaged in tree work appear to have contracted the disease [7].

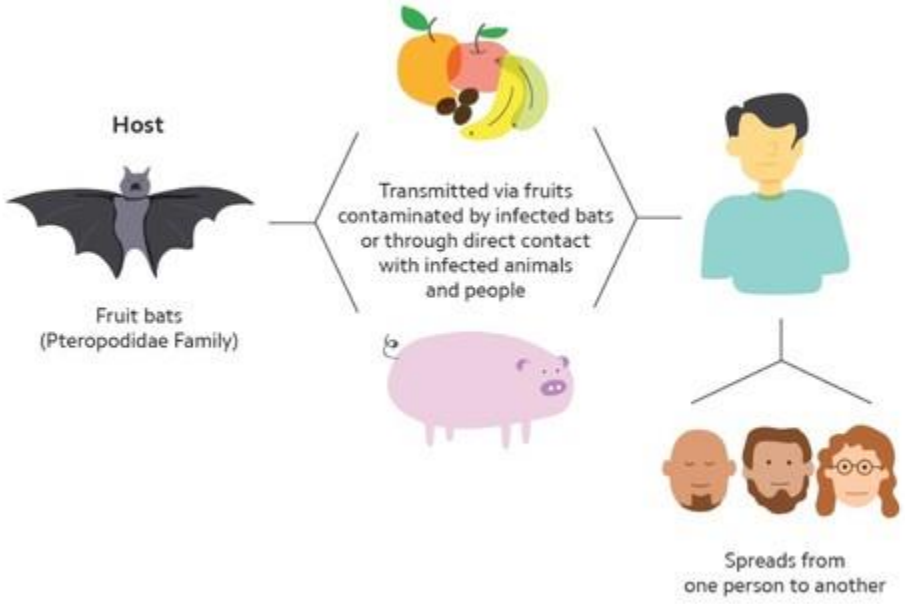

Figure 1.2.1: Virus spread from one person to another

The Nipah virus moved directly from person to person during subsequent epidemics in Bangladesh and India through close contact with human secretions and excretions. About half of the cases that have been documented in Bangladesh since 2001 are the result of close human contact. The majority of these diseases were spread through a limited number of human transmitters, one of which was connected to 22 additional human cases [8].

1.3 Lesions

Different pathogenic characteristics have been seen in humans, particularly at the level of the central nervous system. Confirmed NiV patients displayed prominent vasculitis with endothelial damage, in the arterioles, up to cellular lyses, venules, and capillaries of several organs. The organ most seriously impacted was the brain [9]. In one study, microscopic characteristics in the CNS were evaluated at autopsy and revealed necrotic lesions, perivascular cuffing, thrombosis, and vasculitis in 80% to 90% of the 30 cases examined; endothelial syncytia were present in 27% of the cases, and meningitis was present in 57% of the patients [10]. Additionally, Magnetic Resonance Imaging (MRI) examination of encephalitis patients in the Malaysian outbreak provided evidence of the severity of the CNS disease [11,12]. Heart, lung, and kidney were further affected organs [9,10]. During the outbreaks in Bangladesh, the respiratory illness was observed in up to 63% of confirmed cases [13].

1.4 Symptoms

The incubation phase typically lasts four days to two weeks, although it can be prolonged for 45 to 60 days. The clinical course is marked by a high fever, which is followed by a seizure and death from encephalitis or a respiratory illness. Human infections can range from mild illnesses to deadly encephalitis. Initial flu-like symptoms infected individuals experience include a high fever, headache, myalgia, sore throat, and weakness. Acute encephalitis-related neurological symptoms, such as altered consciousness, atypical sleepiness, and neurological indications that can be accompanied by nausea and vomiting, can occur after this. Atypical pneumonia and serious respiratory issues, including acute respiratory distress, can also be experienced by some patients who are infected with the NiV Bangladesh strain. Septicaemia, gastrointestinal bleeding, and renal failure can all occur in severely affected people. Severe cases might include encephalitis, convulsions, and coma within 24 to 48 hours. During occasional outbreaks, the estimated case fatality rate is 40 to 100%[table]. Acute encephalitis survivors generally make a full recovery, but about 20% of them are left with persistent neurological effects like ongoing convulsions and personality changes [14]. A small percentage of patients who have recovered may develop encephalitic relapse years later, and subclinically infected people may exhibit central nervous system symptoms up to 4 years later [15].

1.5 Diagnosis

Since the initial Nipah virus symptoms are ambiguous, the diagnosis is frequently missed at the time of presentation. This can make it difficult to provide an accurate diagnosis and presents problems with outbreak identification, timely and efficient infection control measures, and activities related to outbreak response. The accuracy of laboratory results can also be impacted by the quantity, quality, timing, type, collection of clinical samples, and time required to transmit samples to the lab. The acute and convalescent phases of the disease allow for the diagnosis of nipah virus infection based on clinical history. The two primary tests are enzyme-linked immunosorbent assays for detecting antibodies and real-time polymerase chain reaction (RT-PCR) from physiological fluids (ELISA). Additionally, the polymerase chain reaction (PCR) assay and virus isolation by cell culture are techniques that are used [16].

1.6 Treatment

Nipah virus infection in humans or animals cannot currently be treated with antiviral medications or vaccinations. The basic strategy for addressing the infection in people is intensive supportive care along with symptom management. In an animal model using ferrets, experimental results showed promise for the therapeutic application of a neutralizing human monoclonal antibody, the m102.4, which targets the receptor binding region of the NiV G glycoproteins. In Non-Human Primate (NHP) animals, the m102.4 was also effectively evaluated against a challenge with the related Hendra virus [17].

1.7 Prevention

Due to the lack of a viable vaccine and chemotherapeutic medicines, prevention of Nipah virus infection is of utmost importance. Avoiding contact with sick pigs and bats in endemic areas is one of the disease prevention techniques. It is best to avoid consuming fruits that have been partially consumed by bats, raw palm sap (palm toddy), open well water that has been contaminated with bat colonies, and raw palm sap that has been treated with bat excrement. Although its potential for use in humans has not been investigated, a subunit vaccine is already available and used in monkeys to protect against the Hendra virus. This vaccine uses the Hendra G protein, which was found to induce cross-protective antibodies against Henipa virus and Nipah virus [18].

1.8 Morphology

A negative-sense, single-stranded RNA virus with an envelope, Nipah has a genome made up of roughly 18,000 nucleotides. The RNA polymerase gene, the nucleocapsid gene (N, P, and L), the envelope membrane protein gene (F and G), and the matrix protein (M) make up the six key genes that make up the structure of the NiV genome. The two membrane-anchored envelope glycoproteins involved in NiV host cell infection are attachment (G) glycoprotein, which contacts the viral receptor, and fusion (F) glycoprotein, which promotes virus-host cell membrane fusion. [19]. Pleomorphic viruses have diameters between 40 and 600 nm. They contain a single layer of surface 246 projections with an average length of 17±1 nm [20].

1.9 Genetic Diversity

The Nipah virus has two important genetic lineages that are known to harm in humans: (1) Nipah Virus- Malaysia (NiV MY), and (2) Nipah Virus- Bangladesh (NiV-BD) [21].

1.10 Genome Size and Structure

The Bangladesh Nipah virus contains 18,252 nucleotides in its genome, compared to the 18,246 nucleotides in the genome of the Malaysia Nipah virus. The role that this increase in viral pathogenicity and interhost transmission might have yet to be discovered. Although the two strains are almost identical in terms of functionality, current research on animal infection suggests that the two viruses may differ in certain respects. NiV-BD is more harmful than NiV-MY, according to infection investigations in the African green monkey, and the window for passive antibody treatment is smaller for NiV-BD [22].

1.11 Sequence of Nipah Virus Polyprotein

The Nucleoprotein (N-protein) of Nipah virus has a molecular mass of 58,168 Dalton and consists of 532 amino acids. The amino acid sequence of N-protein of Nipah virus is as follows:

MSDIFEEAASFRSYQSKLGRDGRASAATATLTTKIRIFVPATNSPELRWELTLFALDVIRS
PSAAESMKVGAAFTLISMYSERPGALIRSLLNDPDIEAVIIDVGSMVNGIPVMERRGDKA
QEEMEGLMRILKTARDSSKGKTPFVDSRAYGLRITDMSTLVSAVITIEAQIWILIAKAVTA
PDTAEESETRRWAKYVQQKRVNPFFALTQQWLTEMRNLLSQSLSVRKFMVEILIEVKK
GGSAKGRAVEIISDIGNYVEETGMAGFFATIRFGLETRYPALALNEFQSDLNTIKSLMLLY
REIGPRAPYMVLLEESIQTKFAPGGYPLLWSFAMGVATTIDRSMGALNINRGYLEPMYF
RLGQKSARHHAGGIDQNMANRLGLSSDQVAELAAAVQETSAGRQESNVQAREAKFAA
GGVLIGGSDQDIDEGEEPIEQSGRQSVTFKREMSISSLANSVPSSSVSTSGGTRLTNSLLNL
RSRLAAKAAKEAASSNATDDPAISNRTQGESEKKNNQDLKPAQNDLDFVRADV

1.12 Family & Domains

Table 1.12.1: Showing features for region, compositional bias

Type	Description	Position	Amino Acid Sequence
Region	Disordered	422-444	IGGSDQDIDEGEEPIEQSGRQSV
	Disordered	487-532	AAKEAASSNATDDPAISNRTQGES EKKNNQDLKPAQNDLDFVRADV
Compositional bias	Basic and acidic residues	510-532	SEKKNNQDLKPAQNDLDFVRADV

Chapter 2

PURPOSE OF THE STUDY

2. Purpose of the study

To determine the N protein of the Nipah Virus in an in silico approach and identifying, investigating and explaining the top 21 ligands that can be used as a potential new Anti-nipah viral drug. This study will illustrate the structure of the N-protein in silico method which will further identify the possible targets for an Anti-Nipah viral drug.

Chapter 3

MATERIALS & METHODS

3. Materials and Methods

In this research, the following materials have been used:

- Protein Data Bank (RCSB-PDB)
- UniProt Knowledgebase (UniProt KB)
- Iterative Threading ASSEmbly Refinement (i-TASSER)
- Ramachandran Plot Assessment (RAMPAGE)
- UCSF Chimera (version 1.13.1)
- Computed Atlas of Surface Topography of Proteins (CASTp)
- e-LEA3D web server
- Mobyle RPBS web portal

The below-mentioned methods were used in this research:

- ab-initio modelling
- Ramachandran plot analysis
- Structure energy minimization
- Determination of ligand binding pocket
- Ligand design
- Determination of the pharmacokinetic property of ligand

Chapter 4

PROCERURE & RESULT

4. Procedure & Results

4.1 Methods for Molecular Modelling of Nipah Virus

UniProt is a widely used database that provides the scientific community with a comprehensive, high-quality and freely accessible resource of protein sequence and functional information. It has been feasible to save a lot of knowledge about how proteins work biologically with the assistance of research publications. This database may be used to determine the target sequence of a protein.

4.1.1 ab-initio Modelling

4.1.1.1 i-TASSER Modeling

The i-TASSER server was visited in the initial phase of ab-initio modeling for makes use of amino acid sequences to predict the 3-D structure of protein molecules. The full-length sequence of the N-protein of the Nipah virus was entered into the i- TASSER server, which resulted in the prediction of five full-length structures of the N-protein of the Nipah virus. The ribbon structures of all five anticipated models, as determined by the UCSF Chimera program, are shown below:

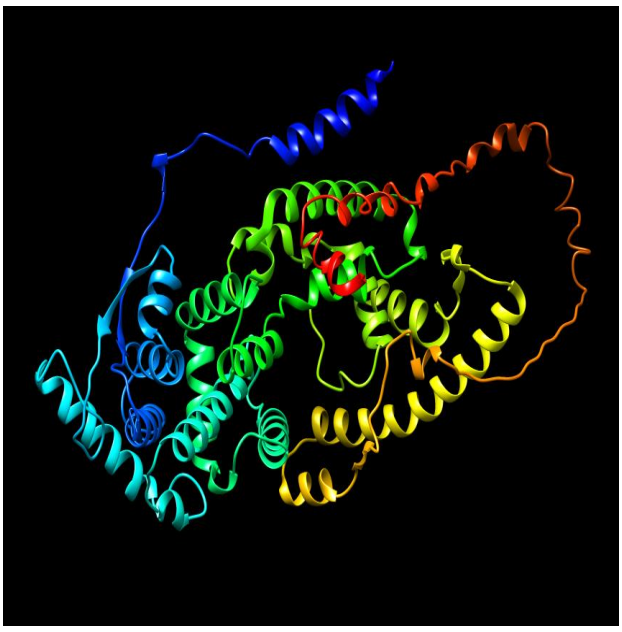

Model 1

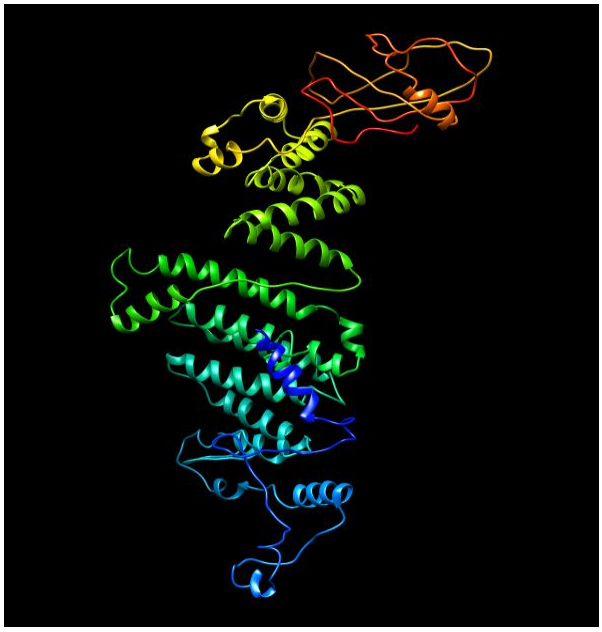

Model 2

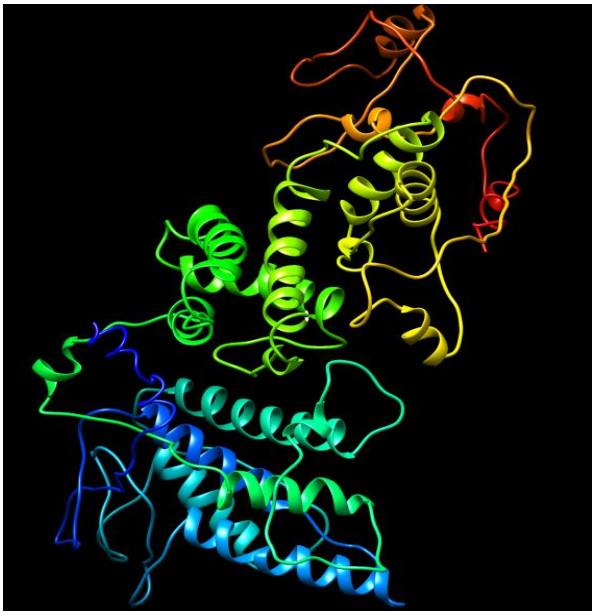

Model 3

Model 4

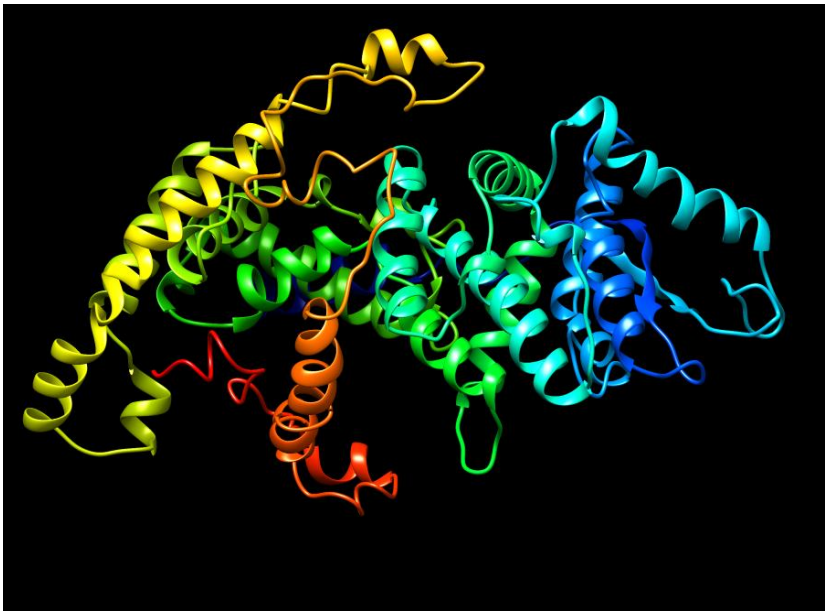

Model 5

Figure 4.1.1.1: Ribbon structures of the predicted models from the i-TASSER server

4.1.1.2 Ramachandran Plot Analysis

In order to perform Ramachandran plot analysis for each of the model structures, the five projected models from the i-TASSER server are submitted and accessed by the RAMPAGE server. Ramachandran plot assessment will provide the favoured region (FR), allowed region (AR), and outlier region (OR) for each and every model structure.

Table 4.1.1.2: Ramachandran plot assessment of all 5 predicted models

Model Number	Favoured Region (FR)	Allowed Region (AR)	FR+AR	Outlier Region (OR)	Inference
Model 1	87.131	10.338	97.469	2.532	Good
Model 2	84.599	9.916	94.515	5.485	Bad
Model 3	81.224	14.768	95.992	4.008	Bad
Model 4	88.608	8.017	96.625	3.376	Bad
Model 5	89.873	7.806	97.679	2.321	Very Good

Since model 5 has the highest favoured region+allowed region and the least outlier region, it is simply based on the findings above that it has a good interference.

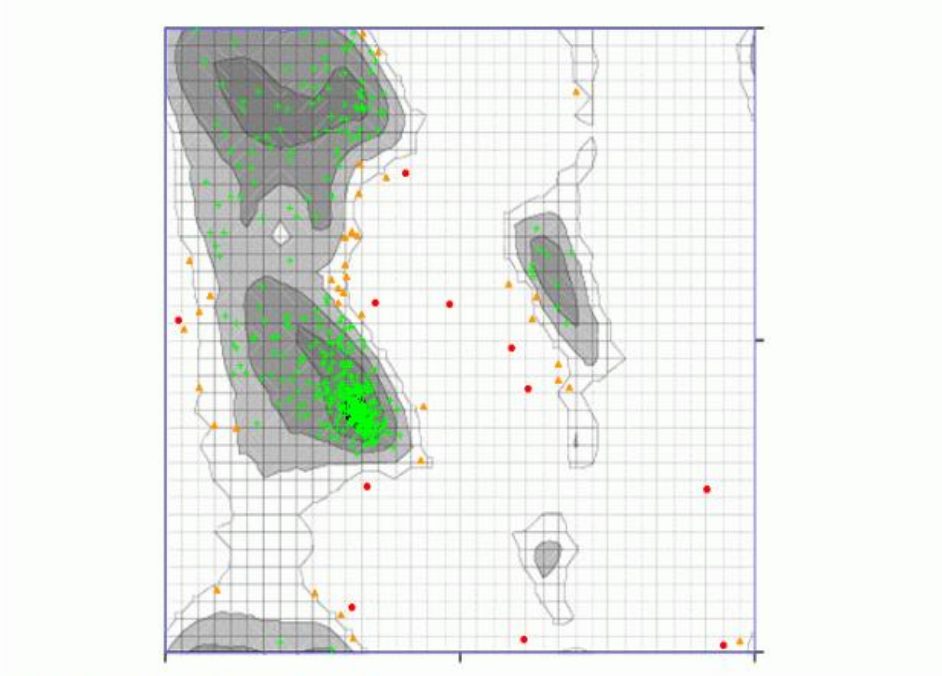

The chart is color-coded for your convenience:

Black Dark Grey Grey Light Grey represent Highly Preferred Conformations. Delta >= -2

White with **Black Grid** represents preferred conformations. -2 > Delta >= -4

White with Grey Grid represents questionable conformations. Delta < -4

Highly Preferred observartions shown as GREEN Crosses: 426 (89.873%)

Preferred observations shown as BROWN Triangles: 37 (7.806%)

Questionable observations shown as RED Circles: 11 (2.321%)

Not Shown: 2

Total: 474

Figure 4.1.1.2: Ramachandran plot analysis report of i-TASSER predicted model 5

4.2 Structure Energy Minimization

A tool called Swiss-PDB Viewer has a user-friendly interface that enables simultaneous analysis of many proteins. To compare active sites or other important components and determine structural alignments, the proteins can be overlaid. Swiss3-PDB Viewer involve calculating and displaying hydrogen bonds, as well as utilizing the Gromos force field to execute energy minimizations [23].

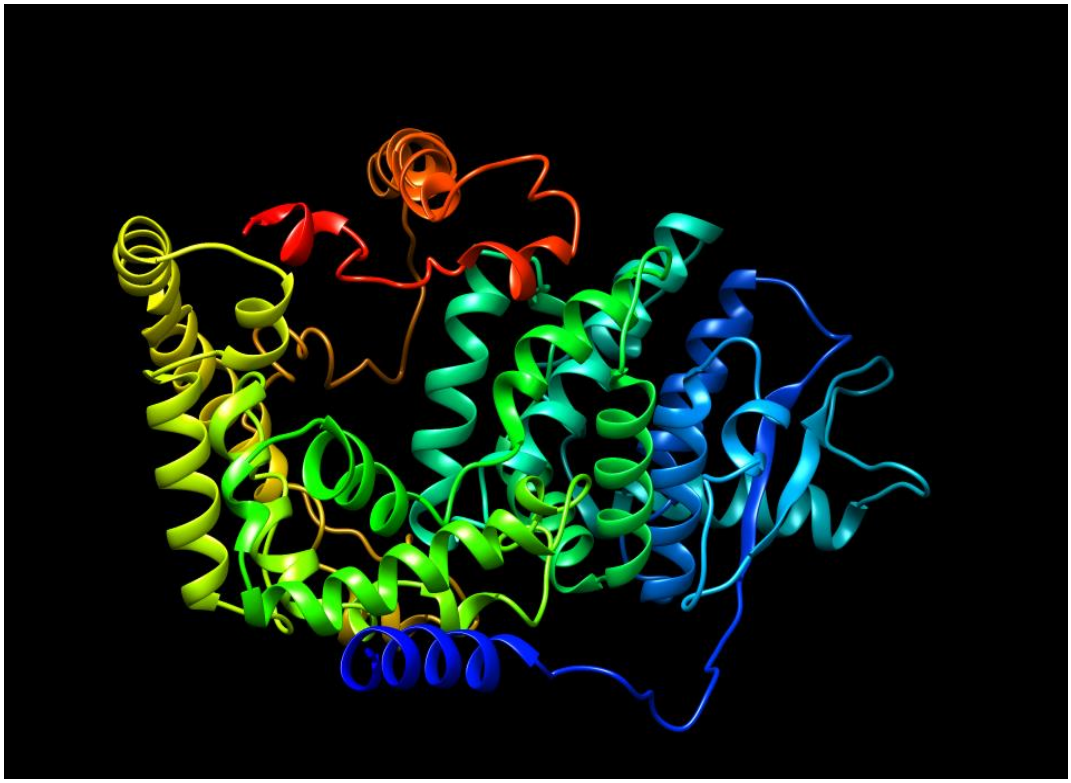

Figure 4.2: Full-length structure of the N- protein of Nipah Virus after energy minimization of model 5

4.3 Ligand Binding Pocket Determination

Ligand binding pockets were established once energy was minimized and the large (L) protein of the Nipah virus was uploaded to the CASTp server in the PDB format. After the CASTp server has identified all of the pockets, only those pockets with an MS volume of less than 1000 but greater than 50 and number of openings is 1that are selected for further experimentation. Then, they are arranged in order of MS pocket area value, highest to lowest. This shortlist of 8 pockets was created. A total of 8 pockets were narrowed down.

The binding site coordinates (x, y, and z) for each of those 8 pockets are determined using the UCSF Chimera software and are listed below:

Table 4.3: Binding site coordinate (x, y, z) determination of 8 pockets

ID	MS Volume	Pocket MS Area	Mouth MS Area	#openings	MS Circumference Sum	X	Y	Z
4	398.6	299.8	63	1	35.5	54.766	69.726	92.127
5	164.9	83.1	95.9	1	46.3	76.868	96.486	47.653
7	141.5	142.6	10.2	1	12.4	55.221	68.009	101.806
8	96.3	97.6	31.6	1	21.5	67.915	94.086	59.317
10	112.9	132.2	26.3	1	20.5	72.294	93.943	52.98
12	94.6	109.5	18.5	1	16.8	69.837	64.959	104.069
13	57.2	62.9	22.4	1	17.6	62.54	57.386	87.062
20	63.9	83.5	12.2	1	13.2	64.776	56.593	91.465

4.4 Ligand Design

The ligands that will bind to the binding sites of the pockets, which were previously identified using the CASTp web server. Ligands are designed using the e-LEA3D server. For each of the N-protein of the Nipah virus's energy-minimized structures, a ligand molecule is produced.

Ligand Design steps mention below:

visiting to the e-LEA3D web server's

http://chemoinfo.ipmc.cnrs.fr

Select ‘Drug design or Screen’ and ‘Enter’

Upload the energy-minimized structure of the protein in PDB format

Insert binding site coordinates (x, y, z) value

Input the value of Binding site radius is “3”

Input the value of Weight in final score is “1”and click ‘Submit’

On the next page enter the email address and choose "De-novo Drug Design" on the next page.

Click on ‘submit’ and the final submission will be completed

The results for all 8 ID will then be sent to the provided email address by the e-LEA3D server. It will produce 21 ligands for each ID, which will then be arranged once more in descending order according to each ligand's best energy score and binding affinity percentage (%).

Table 4.4.1: Ligand design of ID 4 and 5

ID 4			ID 5		
Ligands(Generation number)	**Score of Binding Affinity (%)**	**Best Score of Energy**	**Ligands(Generation number)**	**Score of Binding Affinity (%)**	**Best Score of Energy**
Gen18	80.44	-120.66	Gen18	84.88	-127.320
Gen11	79.17	-118.750	Gen19	81.35	-122.02
Gen12	79.15	-118.73	Gen20	80.17	-120.25
Gen16	79.04	-118.56	Gen16	79.01	-118.52
Gen19	78.91	-118.36	Gen17	78.86	-118.290
Gen20	77.58	-116.37	Gen13	77.13	-115.69
Gen14	77.4	-116.1	Gen14	74.51	-111.77
Gen15	77.28	-115.92	Gen15	72.27	-108.41
Gen13	76.76	-115.14	Gen12	72.08	-108.12
Gen10	75.25	-112.88	Gen11	69.53	-104.3
Gen09	73.87	-110.81	Gen10	69	-103.5
Gen08	73.06	-109.59	Gen09	68.57	-102.85
Gen17	71.83	-107.74	Gen08	68.45	-102.67
Gen07	70.35	-105.52	Gen05	68.2	-102.3
Gen03	69.87	-104.81	Gen06	65.82	-98.73
Gen06	68.13	-102.2	Gen07	65.82	-98.73
Gen05	66.69	-100.03	Gen04	62.76	-94.14
Gen04	66.16	-99.24	Gen03	55.99	-83.99
Gen02	63.71	-95.56	Gen02	55.17	-82.76
Gen01	59.91	-89.86	Gen01	53.19	-79.78
Gen00	52.56	-78.84	Gen00	49.63	-74.45

Table 4.4.2: Ligand design of ID 7 and 8

ID 7			ID 8		
Ligands(Generation number)	**Score of Binding Affinity (%)**	**Best Score of Energy**	**Ligands(Generation number)**	**Score of Binding Affinity (%)**	**Best Score of Energy**
Gen16	81.81	-122.72	Gen17	76.46	-114.69
Gen18	78.55	-117.82	Gen15	75.89	-113.84
Gen19	76.89	-115.33	Gen12	75.59	-113.39
Gen14	76.17	-114.26	Gen11	75.28	-112.92
Gen15	75.35	-113.03	Gen14	74.51	-111.76
Gen17	74.29	-111.43	Gen18	74.09	-111.13
Gen20	72.37	-108.56	Gen20	72.63	-108.95
Gen12	72.02	-108.03	Gen19	71.8	-107.7
Gen13	69.13	-103.69	Gen08	71.77	-107.660
Gen11	68.64	-102.96	Gen10	71.73	-107.6
Gen10	63.54	-95.31	Gen16	70.13	-105.19
Gen09	60.55	-90.82	Gen09	69.03	-103.54
Gen08	58.53	-87.8	Gen07	67.88	-101.82
Gen07	55.75	-83.62	Gen13	67.87	-101.8
Gen06	53.69	-80.54	Gen05	65.44	-98.16
Gen05	53.35	-80.02	Gen06	65.03	-97.54
Gen02	50.04	-75.06	Gen04	64.64	-96.96
Gen01	50.03	-75.05	Gen02	63.56	-95.34
Gen03	49.24	-73.86	Gen03	58.13	-87.2
Gen04	48.17	-72.25	Gen01	53.69	-80.53
Gen00	42.18	-63.27	Gen00	51.93	-77.900

Table 4.4.3: Ligand design ID 10 and 12

ID 10			ID 12		
Ligands(Generation number)	**Score of Binding Affinity (%)**	**Best Score of Energy**	**Ligands(Generation number)**	**Score of Binding Affinity (%)**	**Best Score of Energy**
Gen15	94.51	-141.77	Gen19	68.93	-103.39
Gen18	91.61	-137.41	Gen11	66.35	-99.52
Gen20	90.03	-135.05	Gen17	65.43	-98.15
Gen17	88.53	-132.79	Gen18	65.19	-97.78
Gen19	88.29	-132.44	Gen16	64.67	-97
Gen12	86.16	-129.24	Gen15	63.79	-95.68
Gen16	85.3	-127.95	Gen13	63.56	-95.34
Gen14	84.46	-126.69	Gen14	62.62	-93.93
Gen11	83.19	-124.79	Gen12	61.63	-92.44
Gen13	82.92	-124.38	Gen10	56.75	-85.13
Gen10	82.46	-123.69	Gen07	56.17	-84.26
Gen09	78.57	-117.86	Gen08	56.16	-84.240
Gen08	71.3	-106.95	Gen09	56.15	-84.23
Gen07	70.24	-105.36	Gen06	56.09	-84.14
Gen06	68.51	-102.76	Gen05	54.02	-81.03
Gen04	66.18	-99.27	Gen04	54	-81
Gen05	61.45	-92.17	Gen01	49.35	-74.02
Gen03	60.62	-90.93	Gen03	49.35	-74.02
Gen01	54.05	-81.07	Gen00	49.34	-74.01
Gen02	53.77	-80.66	Gen02	49.34	-74.01
Gen00	52.38	-78.57			

Table 4.4.4: Ligand design ID 13 and 20

ID 13			ID 20		
Ligands(Generation number)	**Score of Binding Affinity (%)**	**Best Score of Energy**	**Ligands(Generation number)**	**Score of Binding Affinity (%)**	**Best Score of Energy**
Gen20	75.59	-113.38	Gen20	83.81	-125.72
Gen19	74.18	-111.27	Gen19	79.77	-119.65
Gen18	73.39	-110.09	Gen18	80.69	-121.03
Gen17	72.07	-108.1	Gen17	83.98	-125.97
Gen15	69.27	-103.91	Gen15	79.79	-119.68
Gen16	69.15	-103.73	Gen16	78.57	-117.85
Gen10	67.73	-101.59	Gen10	59.54	-89.31
Gen09	67.4	-101.1	Gen09	59.01	-88.52
Gen12	67.25	-100.88	Gen12	67.61	-101.41
Gen13	67	-100.5	Gen13	67.61	-101.42
Gen11	66.5	-99.75	Gen11	61.31	-91.96
Gen08	65.64	-98.46	Gen08	58.39	-87.58
Gen14	63.62	-95.43	Gen14	76.75	-115.12
Gen07	60.84	-91.26	Gen07	55.29	-82.94
Gen06	59.88	-89.82	Gen06	54.06	-81.09
Gen05	57.06	-85.59	Gen05	53.89	-80.83
Gen04	54.67	-82.01	Gen04	53.67	-80.51
Gen03	49.82	-74.73	Gen03	51.51	-77.26
Gen02	49.07	-73.6	Gen02	51.47	-77.21
Gen01	48.1	-72.15	Gen01	46.57	-69.85
Gen00	43.52	-65.28	Gen00	46.57	-69.85

The structure of the ligand molecules in each pocket with the highest percentage of binding affinity and the best of energy score is provided below:

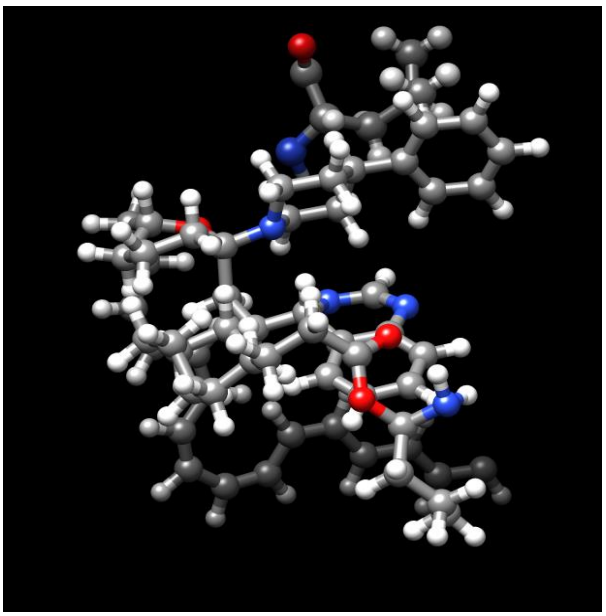

Pocket ID 4 Generation 18

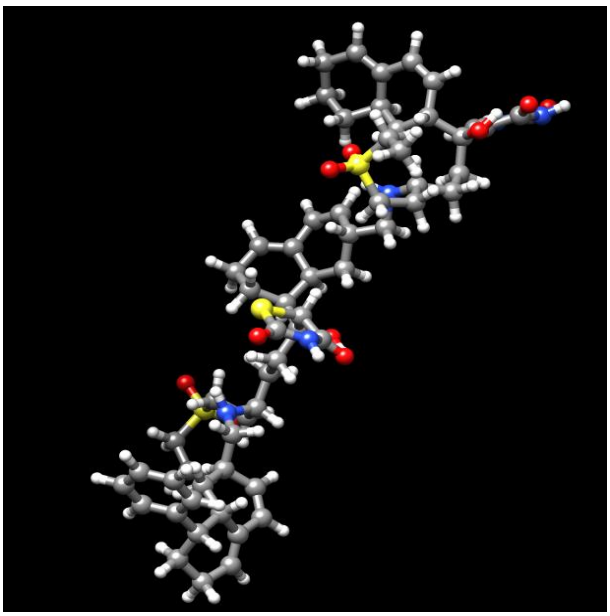

Pocket ID 5 Generation 18

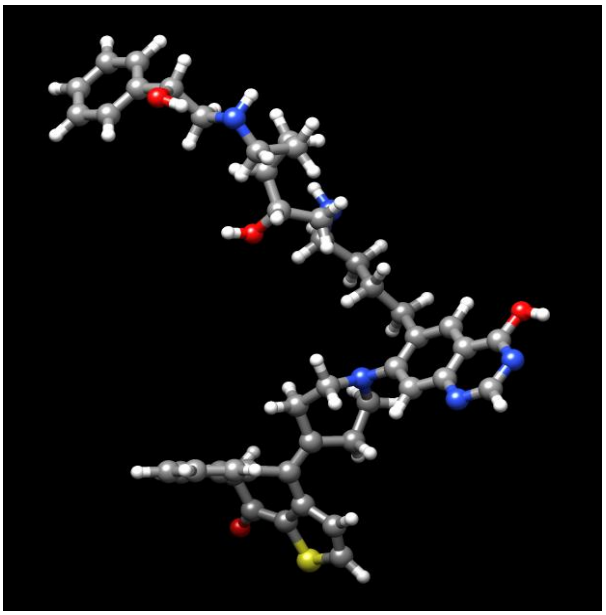

Pocket ID 7 Generation 16

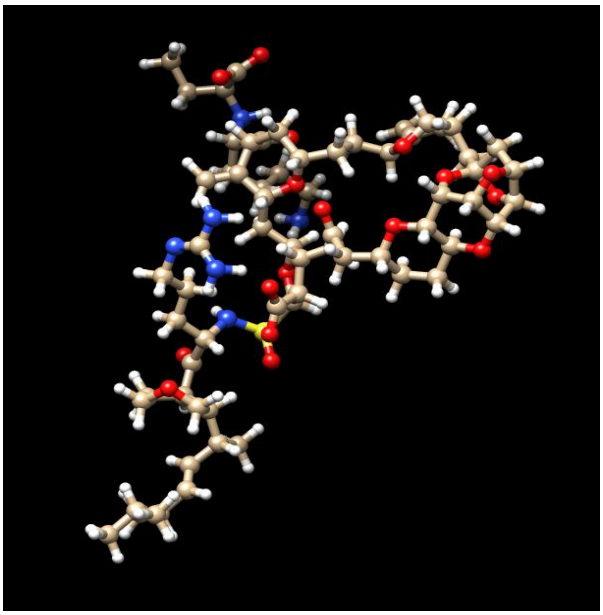

Pocket ID 8 Generation 17

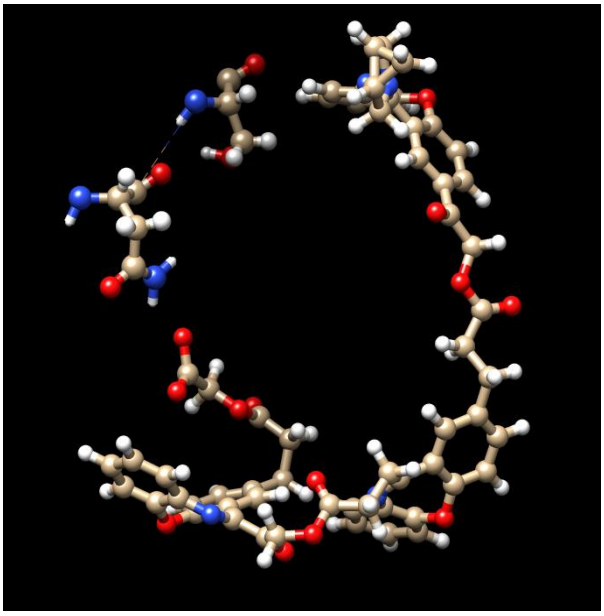

Pocket ID 10 Generation 15

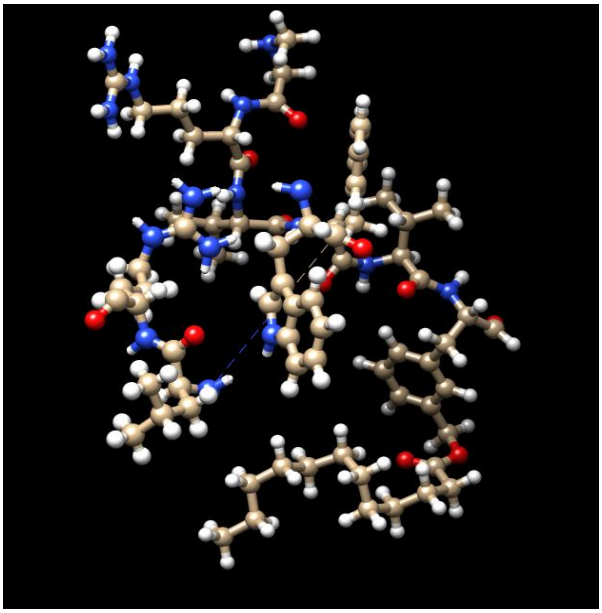

Pocket ID 12 Generation 19

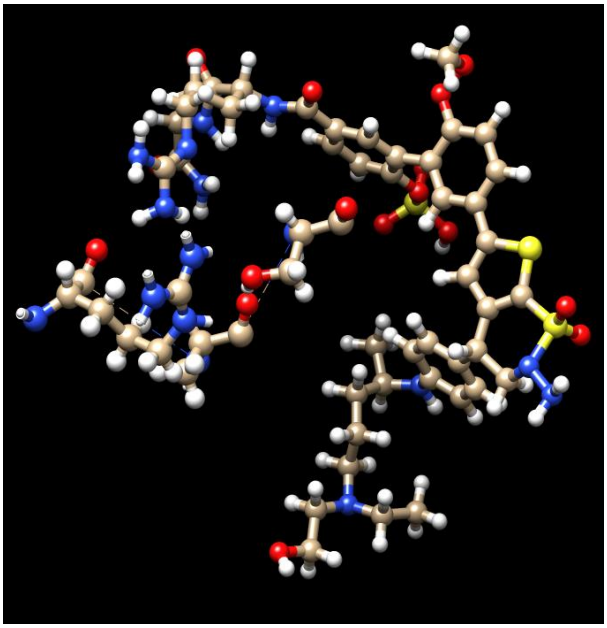

Pocket ID 13 Generation 19

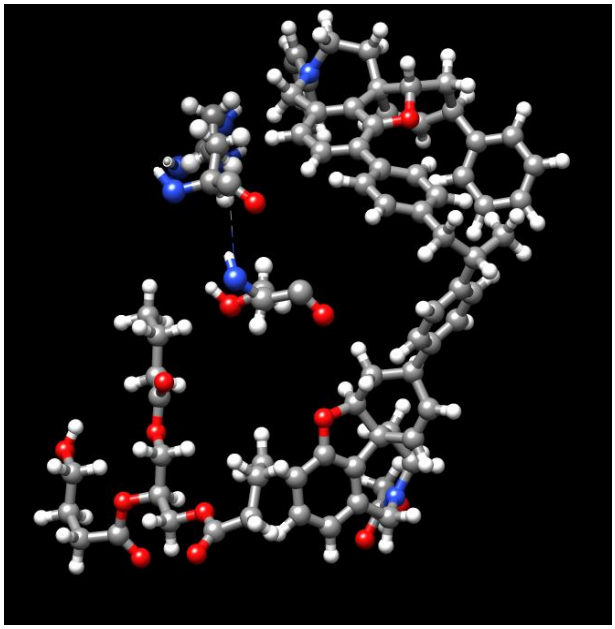

Pocket ID 20 Generation 20

Figure 4.4: 3D Structure of Ligand Molecules

4.5 Determination of Ligand Pharmacokinetic Properties

The Mobyle RPBS web site can be used to identify the pharmacokinetic properties of ligand molecules after they have been created via the e-LEA3D server. Each of the N- protein pockets ligand molecules were evaluated for its pharmacokinetic characteristics, steps mention below:

Visit the RPBS web portal at

http://mobyle.rpbs.univ-paris-diderot.fr/cgibin/portal.py#welcome

↓

Go to the 'Programs' menu and select 'Drugs'

↓

Then select 'FAF-Drugs4' option and the following 'FAF-Drugs4' option as well

↓

In the 'Demonstration mode' menu, choose 'No' for test the service with server sample data

↓

Select "Upload" and then pick the sdf file containing the ligand molecules for each pocket in the "Input data" window.

↓

In the 'logP method' menu, select 'XLOGP3' for logP computation program

↓

In the 'Filtering options' window

- In house [*] and published physchem filters [+], Select 'No'
- PPIHitProfiler (Sperandio et. al.), Select 'No'
- Filter undesirable substructures moieties, Select 'No'
- Retrieve covalent inhibitors, Select 'No'
- Filter Pan Assay Interference Compounds (PAINS) Filter A, Select 'Yes'
- Filter Pan Assay Interference Compounds (PAINS) Filter B, Select 'Yes'
- Filter Pan Assay Interference Compounds (PAINS) Filter C, Select 'Yes'
- Lilly MedChem Rules (only detection, no triage), Choose 'regular'

↓

Scroll up on top of the web page and to submit, click 'Run

After finishing the submission, I will get the pharmacokinetic properties of best ligands for all of the ID, which is given below:

Table 4.5.1: Pharmacokinetic Properties of all 8 pocket

ID	Ligands (Generation Number)	MW	logP	logD	logSw	tPSA	Rotatable Bonds	Rigid Bonds
4	Gen18	853.23	14.4	10.82	-14.07	91.99	3	64
5	Gen18	1142.5	7.49	-0.35	-10.05	299.48	25	58
7	Gen16	745.97	6.02	1.95	-7.38	168.24	16	41
8	Gen17	1299.61	-1.69	-1.82	-5.31	379.35	23	66
10	Gen15	1021	7.29	5.41	-9.59	221.18	21	64
12	Gen19	934.22	7.2	1.48	-7.85	269.12	36	25
13	Gen19	1003.2	-0.48	-6.19	-4.24	397.29	25	39
20	Gen20	1173.4	12.42	11.98	-13.45	161.37	25	69

Table 4.5.1: Pharmacokinetic Properties of all 8 pocket (continued)

ID	Ligands (Generation Number)	Flexibility	HB Donnors	HB Acceptors	HBD_HBA	Rings	Max Size Ring
4	Gen18	0.04	3	7	10	4	40
5	Gen18	0.3	7	15	22	6	10
7	Gen16	0.28	5	9	14	4	14
8	Gen17	0.26	10	24	34	2	47
10	Gen15	0.25	1	17	18	4	15
12	Gen19	0.59	10	17	27	2	6
13	Gen19	0.39	13	22	35	4	9
20	Gen20	0.27	2	13	15	6	17

Table 4.5.1: Pharmacokinetic Properties of all 8 pocket (continued)

ID	Ligands (Generation Number)	Charge	Total Charge	Heavy Atoms	Carbon Atoms	Hetero Atoms	Ratio H/C	Lipinski Violations
4	Gen18	2	2	63	56	7	0.13	2
5	Gen18	2	2	79	61	18	0.3	4
7	Gen16	2	2	54	44	10	0.23	2
8	Gen17	5	1	91	66	25	0.38	3
10	Gen15	1	-1	76	59	17	0.29	3
12	Gen19	2	2	67	50	17	0.34	4
13	Gen19	3	1	68	43	25	0.58	3
20	Gen20	0	0	87	74	13	0.18	3

Table 4.5.1: Pharmacokinetic Properties of all 8 pocket (continued)

ID	Ligands (Generation Number)	Solubility (mg/l)	Solubility Forecast Index	Oral Bioavailability (VEBER)	Oral Bioavailability (EGAN)	Traffic Lights
4	Gen18	0.66	Reduced Solubility	Good	Good	4
5	Gen18	49.48	Good Solubility	Low	Low	8
7	Gen16	462.93	Reduced Solubility	Low	Low	8
8	Gen17	6391.28	Good Solubility	Low	Good	6
10	Gen15	69.71	Reduced Solubility	Low	Low	8
12	Gen19	363.03	Good Solubility	Low	Low	8
13	Gen19	14504.11	Good Solubility	Low	Good	6
20	Gen20	1.69	Reduced Solubility	Low	Low	8

Table 4.5.1: Pharmacokinetic Properties of all 8 pocket (continued)

ID	Ligands (Generation Number)	4_400	3_75	Phospholipidosis	Fsp3	Stereo Centers	PPI_ Friendly
4	Gen18	bad	warning	Non-Inducer	0.5	7	Not Computed
5	Gen18	bad	warning	Non-Inducer	0.61	13	Not Computed
7	Gen16	bad	warning	Inducer	0.39	2	Not Computed
8	Gen17	good	good	Non-Inducer	0.82	25	Not Computed
10	Gen15	bad	warning	Non-Inducer	0.24	2	Not Computed
12	Gen19	bad	warning	Inducer	0.6	5	Not Computed
13	Gen19	good	good	Inducer	0.4	3	Not Computed
20	Gen20	bad	warning	Non-Inducer	0.41	8	Not Computed

Table 4.5.1: Pharmacokinetic Properties of all 8 pocket (continued)

ID	Ligands (Generation Number)	Status
4	Gen18	Accepted
5	Gen18	Accepted
7	Gen16	Accepted
8	Gen17	Accepted
10	Gen15	Accepted
12	Gen19	Accepted
13	Gen19	Accepted
20	Gen20	Accepted

Finally, the status of each of the ligands of pockets are generated as Accepted, Intermediate, or Rejected following the successful screening of all the properties from the aforementioned table. All of the ligand molecules have been approved according to FAF-Drugs4. According to the results of the FAF-Drugs4 filtering, any ligands with an Accepted status can be synthesized in the lab and, after undergoing a number of laboratory tests (from preclinical to phase 4 of a clinical trial), can be selected as an anti-Nipah medicine.

Chapter 5

CONCLUSION

5. Conclusion

We are aware that X-ray crystallography, despite having excellent precision, is still perceived as a costly and time-consuming method for determining protein structure. As a result, comparative modeling enables us to forecast the structure and expands the field of potential proteins and antiviral drugs. After the i-TASSER successfully generated 3D homology models of the N- protein of the Nipah virus, Ramachandran analysis was used to validate those models. Diagram creation and modification were aided using UCSF Chimera. The CASTp web server was used to help locate the inhibitory sites for the Nipah virus large (L) protein. We anticipate molecular docking of the structures in the pockets in the future based on the results of this experiment, where we hope to find the best-fitting structure that will ultimately help us produce Nipah virus inhibitors.

Chapter 6

REFERENCE

6. Reference

1. Jamaluddin, B. A. A., & Adzhar, B. A. (2011, February). Case story 2: Nipah virus: experience from Malaysia 1998–1999. In OIE Global Conference on wildlife animal health and biodiversity: Preparing for the future. Paris (France) (pp. 23-25).
2. Negrete, O. A., Wolf, M. C., Aguilar, H. C., Enterlein, S., Wang, W., Mühlberger, E., ... & Lee, B. (2006). Two key residues in ephrinB3 are critical for its use as an alternative receptor for Nipah virus. PLoS pathogens, 2(2), e7.
3. Pallister, J., Middleton, D., Broder, C. C., & Wang, L. F. (2011). Henipavirus vaccine development. J Bioterr Biodef S, 1, 2.
4. Institute of Epidemiology, Disease Control and Research (IEDCR). Yearly distribution of Nipah cases in Bangladesh 2001-2021.
5. Rajbari, M., Rajbari, N., & Faridpur, F. Morbidity and mortality due to Nipah or Nipah-like virus encephalitis in WHO South-East Asia Region Country: India 2018; 2018.
6. Hegde, S. T., Sazzad, H., Hossain, M. J., Alam, M. U., Kenah, E., Daszak, P., ... & Gurley, E. S. (2016). Investigating rare risk factors for Nipah virus in Bangladesh: 2001–2012. Ecohealth, 13(4), 720-728.
7. Hughes, J. M., Wilson, M. E., Luby, S. P., Gurley, E. S., & Hossain, M. J. (2009). Transmission of human infection with Nipah virus. Clinical Infectious Diseases, 49(11), 1743-1748.
8. Blum, L. S., Khan, R., Nahar, N., & Breiman, R. F. (2009). In-depth assessment of an outbreak of Nipah encephalitis with person-to-person transmission in Bangladesh: implications for prevention and control strategies. The American journal of tropical medicine and hygiene, 80(1), 96-102.
9. Chua, K. B., Bellini, W. J., Rota, P. A., Harcourt, B. H., Tamin, A., Lam, S. K., ... & Mahy, B. W. J. (2000). Nipah virus: a recently emergent deadly paramyxovirus. Science, 288(5470), 1432-1435.
10. Wong, K. T., Shieh, W. J., Kumar, S., Norain, K., Abdullah, W., Guarner, J., ... & Nipah Virus Pathology Working Group. (2002). Nipah virus infection: pathology and pathogenesis of an emerging paramyxoviral zoonosis. The American journal of pathology, 161(6), 2153-2167.
11. Lim, C. T. (2009). MR imaging in Nipah virus infection. Neurology Asia, 14(1), 49-52.

12. Sarji, S. A., Abdullah, B. J. J., Goh, K. J., Tan, C. T., & Wong, K. T. (2000). MR imaging features of Nipah encephalitis. American Journal of Roentgenology, 175(2), 437-442.
13. Ali, M. Y., Fattah, S. A., Islam, M. M., Hossain, M. A., & Ali, S. Y. (2010). Outbreak of Nipah Encephalitis In Greater Faridpur District. Faridpur Medical College Journal, 5(2), 63-65.
14. World Health Organization (2009) Nipah virus. Media Center. Fact sheet 262.
15. Chong, H. T., & Tan, C. T. (2003). Relapsed and late-onset Nipah encephalitis, a report of three cases. Neurol J Southeast Asia, 8(2), 109-112.
16. World Health Organization. Newsroom. Fact sheet of Nipah virus. 30 May 2018.
17. Bossart, K. N., Geisbert, T. W., Feldmann, H., Zhu, Z., Feldmann, F., Geisbert, J. B., ... & Rockx, B. (2011). A neutralizing human monoclonal antibody protects african green monkeys from hendra virus challenge. Science translational medicine, 3(105), 105ra103-105ra103.
18. Bossart, K. N., Rockx, B., Feldmann, F., Brining, D., Scott, D., LaCasse, R., ... & Geisbert, T. W. (2012). A Hendra virus G glycoprotein subunit vaccine protects African green monkeys from Nipah virus challenge. Science translational medicine, 4(146), 146ra107-146ra107.
19. Lamb, R. A. (2001). Paramyxoviridae: the viruses and their replication. Fields virology.
20. Wang LF, Mackenzie JS, Broder CC. 2013. Henipaviruses. Knipe DM, Howley PM (ed), Lippincott Williams & Wilkins, Philadelphia. Fields Virology 2:286-313.
21. Luby, S. P., Rahman, M., Hossain, M. J., Blum, L. S., Husain, M. M., Gurley, E., ... & Ksiazek, T. G. (2006). Foodborne transmission of Nipah virus, Bangladesh. Emerging infectious diseases, 12(12), 1888.
22. Harcourt, B. H., Lowe, L., Tamin, A., Liu, X., Bankamp, B., Bowden, N., ... & Rota, P. A. (2005). Genetic characterization of Nipah virus, Bangladesh, 2004. Emerging infectious diseases, 11(10), 1594.
23. van Gunsteren, W. F., Billeter, S. R., Eising, A. A., Hünenberger, P. H., Krüger, P. K. H. C., Mark, A. E., ... & Tironi, I. G. (1996). Biomolecular simulation: the GROMOS96 manual and user guide. Vdf Hochschulverlag AG an der ETH Zürich, Zürich, 86, 1-1044.